Chapter 3

Single-Phase Shell-Side Flows and Heat Transfer

SUMMARY: The design method of Taborek (1983) for single-phase shell-side flows of shell-and-tube heat exchangers with *single segmental baffles* is presented here. The Taborek version of the Delaware method is thought to be the most accurate, reliable and complete method available in the open literature. The basic theory of single-phase shell-side flow in baffled heat exchangers is presented and then a complete treatment of the Taborek method for application to plain tubes and integral low finned tubes, such as the Wolverine Tube S/T Trufin tubes. The method predicts both heat transfer coefficients and pressure drops as a function of the tube bundle geometry and its dimensional description.

3.1 Introduction

Single-phase flow of liquids and gases over tube bundles is an important heat transfer process confronted in numerous types of heat exchanger applications. In contrast to single-phase heat transfer inside tubes, shell-side flows (i.e. those across the outside of the tubes in a baffled tube bundle confined by a heat exchanger shell) are particularly complex because of the many geometrical factors involved and the many possible fluid flow paths. Tinker (1951) was the first to give a physical description of this process, which was used in the development of what is often referred to as the *Delaware method*, proposed by Bell (1960, 1963) and republished in Bell (1986). Taborek (1983) proposed a new version of this design method for single-phase shell-side flows of shell-and-tube heat exchangers with single segmental baffles (essentially for what is called a TEMA E-shell) and described how to extended it to TEMA J-shells and F-shells and to E-shells with no-tubes-in-the-window. The basic theory of single-phase shell-side flow in baffled E-shell heat exchangers is presented here and then a more complete treatment of the Taborek method. This method is for flow over tube bundles with *single-segmental baffles*. Other types of baffles used in special applications include double-segmental baffles, triple-segmental baffles, disk-and-donut baffles, rod baffles and helical baffles; these alternative, less used geometries are not addressed here. In this chapter, first the method for *plain tubes* is described and then its extension to *integral low finned tubes*.

3.2 Stream Analysis of Flow Distribution in a Baffled Heat Exchanger

In a baffled shell-and-tube heat exchanger, only a fraction of the fluid flow through the shell-side of a heat exchanger actually flows across the tube bundle in the idealized path normal to the axis of the tubes. The remaining fraction of the fluid flows through "bypass" areas. As can be expected, the fluid seeks the flow path of less resistance from the inlet to the outlet of the exchanger. In a typical design, the *non-ideal* flows represent up to 40% of the total flow and hence it is imperative to account for their effects on heat transfer and pressure drop.

These flow paths in an actual heat exchanger with single-segmental baffles were first intuitively described by Tinker (1951) as depicted in his schematic diagram shown in Figure 3.1. The total flow is divided into individual streams designated by the letters shown in the diagram as follows:

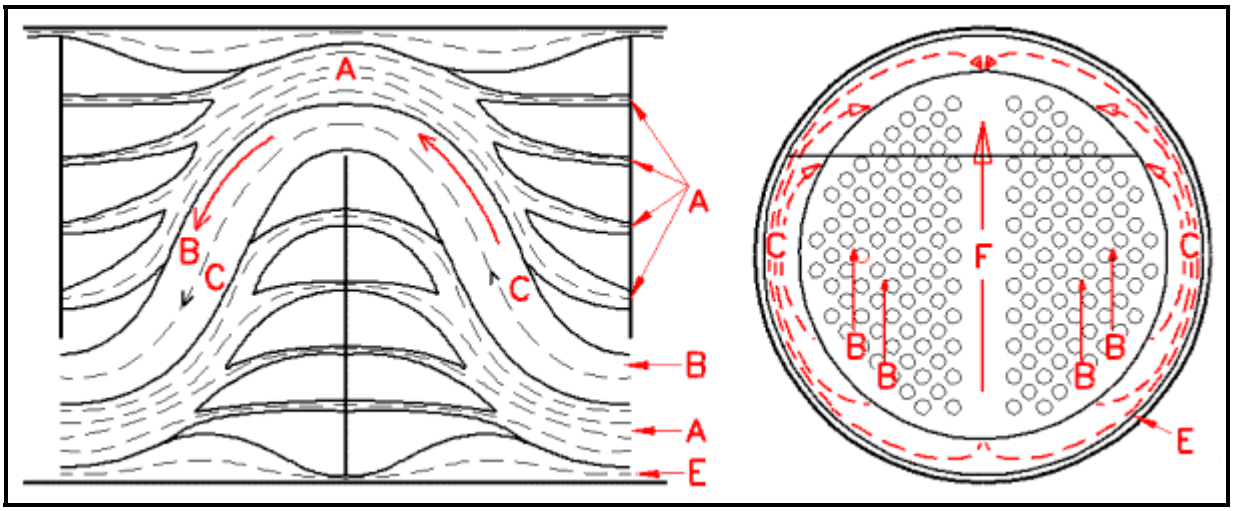

Figure 3.1. Shell-side flow paths in a baffled heat exchanger according to Tinker (1951).

The total flow is divided into individual streams designated by the letters shown in the diagram as follows:

- **Stream A**: The *tube hole leakage stream* represents the flow from one baffle compartment to the next that passes through the annular openings between the oversized holes for the tubes in the baffles and the outside of the tubes, as illustrated in Figure 3.2. The flow is driven by the pressure drop from one baffle compartment to the next. The leakage occurs through the diametral clearance between the diameter of the baffle hole minus the outside diameter of the tube. If the tubes are expanded into the baffles, then the diametral clearance is zero. This bypass stream is minimized by reducing the diametral clearance and completely eliminated if the clearance becomes zero.

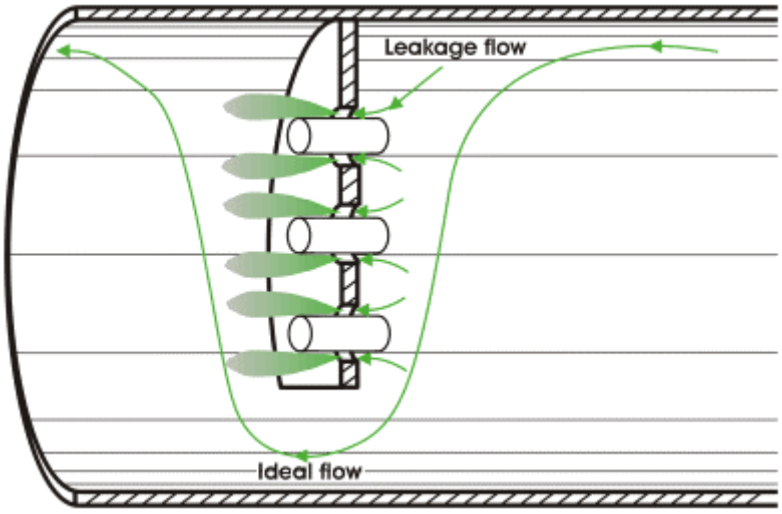

Figure 3.2. Diagram of tube hole leakage stream A.

- **Stream B**: The *crossflow stream* is the idealized cross flow over the tube bundle normal to the axis of the tubes. This is the preferred flow in a baffled shell-and-tube heat exchanger and is illustrated in Figure 3.1.

- **Stream C**: The *bundle bypass stream* flows through the annular opening between the outside of the tube bundle and the inner shell wall as illustrated in Figure 3.3. The diametral clearance for this flow to pass through is equal to the shell internal diameter minus the outer tube limit diameter of the tube bundle. The bundle bypass stream is reduced by minimizing the diametral clearance between the shell internal diameter and the outer tube limit diameter of the tube bundle and by installing pairs of sealing strips around the perimeter of the tube bundle to block this flow path and thereby force the fluid back into the tube bundle.

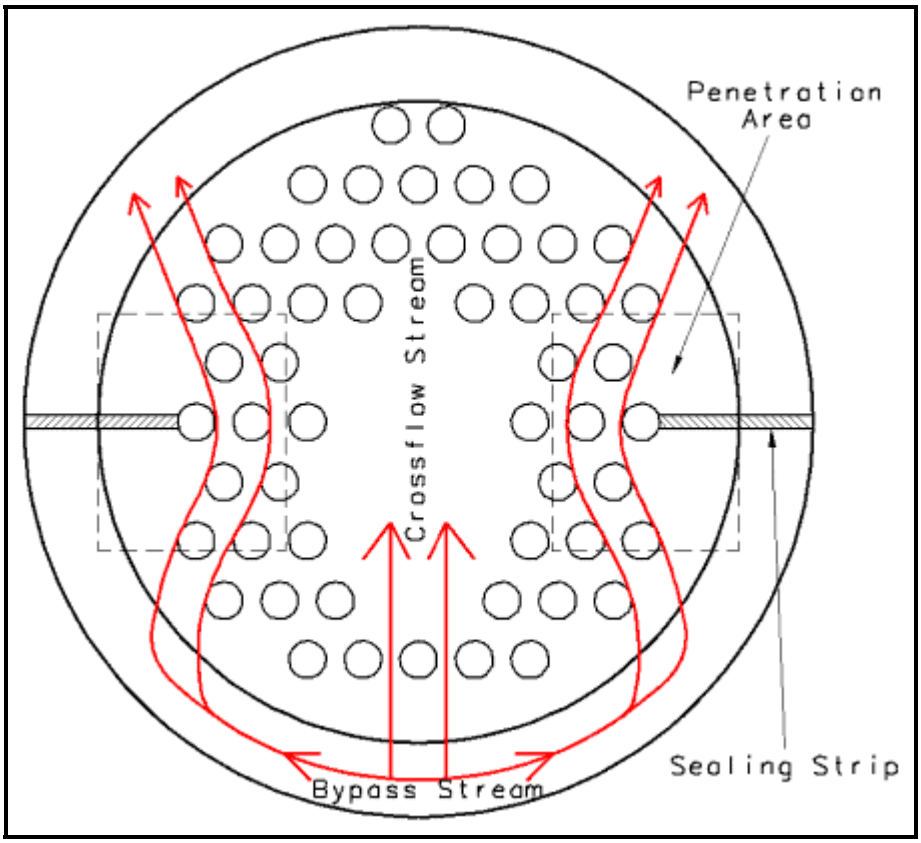

Figure 3.3. Schematic of bundle bypass stream C.

- **Stream E**: The *shell-to-baffle bypass stream* refers to the flow through the gap between the outer edge of the baffle and the inner shell wall as depicted in Figure 3.4. The diametral clearance is equal to the shell internal diameter minus the diameter of the baffle and is minimized by decreasing the construction clearance between the shell and the baffle to its feasible minimum.

- **Stream F**: The *pass partition bypass stream* refers to the flow through the open lanes in a tube bundle formed by omission of tubes in the bundle and tubesheet for placement of tubepass partition plates in the heads of multi-pass heat exchangers. It is illustrated in Figure 3.1. This stream only refers to those openings oriented in the *direction* of the fluid flow. Pass partition openings oriented *normal* to the flow path do *not* cause a bypass. This bypass stream thus only occurs in some multi-pass tube layouts and they can be eliminated by placement of several dummy tubes in each bypass lane to drive the fluid back into the tube bundle.

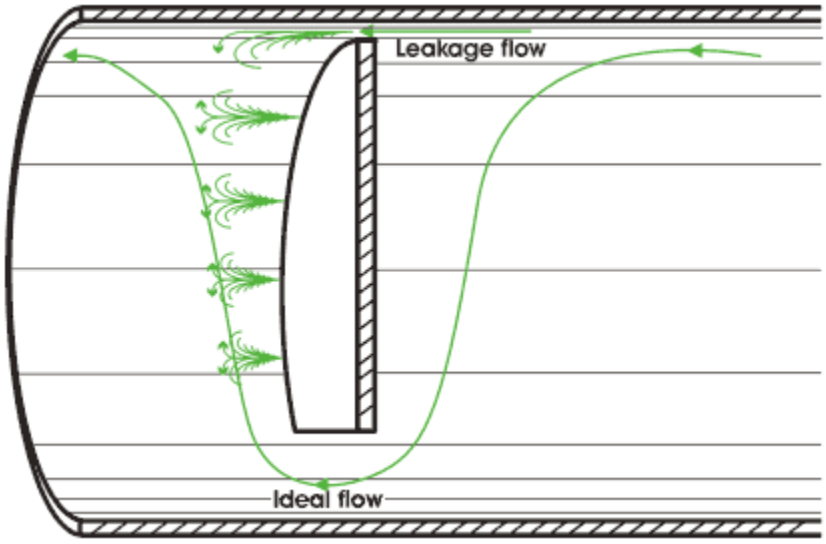

Figure 3.4. Schematic of shell-to-baffle bypass stream E.

3.3 Definition of Bundle and Shell Geometries

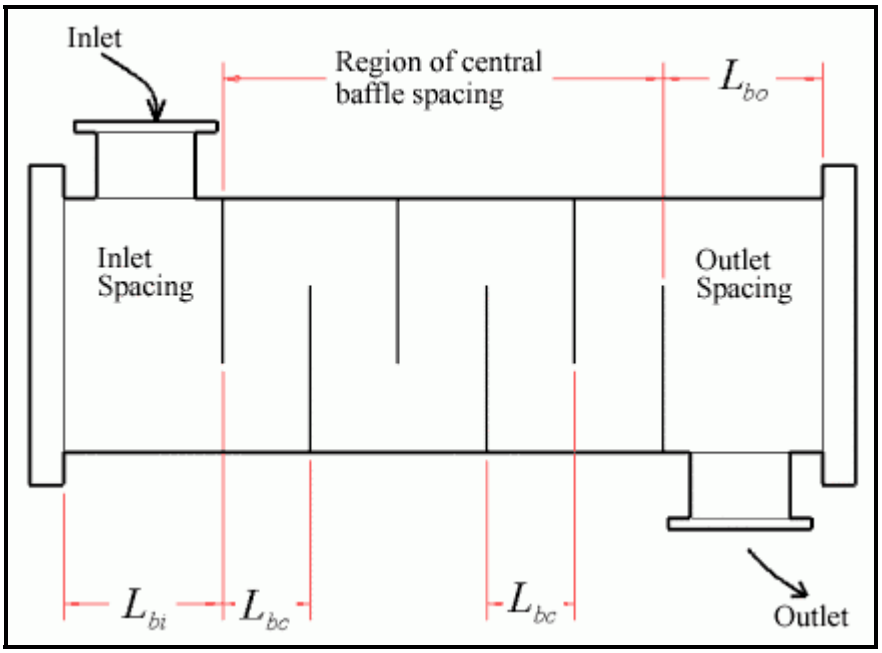

Figure 3.5. Single-segmental shell-and-tube heat exchanger showing baffle spacings.

Figure 3.5 depicts a single-segmental shell-and-tube bundle geometry with fixed tubesheets at both heads in which the shell-side flow makes one shell pass from one end of the tube bundle to the other with the flow directed across the tube bundle by the baffles. This is a common configuration used in refrigeration and petrochemical heat exchangers. The inlet, central and outlet baffle spacings are shown and are identified as L_{bi}, L_{bc} and L_{bo}, respectively. L_{bi} and L_{bo}, are often equal in length to L_{bc}, except when the first and last baffle compartments must be enlarged to allow for the placement of the respective shell-side

nozzles. The baffle layout is determined from the inlet, central, and outlet baffle spacings and the effective tube length. The effective tube length L_{ta} is equal to the total tube length less the combined thickness of the two tubesheets. The number of baffles (an integer) and baffle spacings can be determined from these values. The effective length for determining the baffle spacing for a U-tube exchanger includes the straight length of the tube plus $D_s/2$, where D_s is the shell internal diameter. Thus the baffle spacing at the U-bend should include the tube straight length in this compartment plus ($D_s/2$).

Figures 3.5, 3.6 and 3.7 reproduced from Taborek (1983) define the principal heat exchanger dimensions. D_{otl} is the *o*uter *t*ube *l*imit diameter and D_{ctl} is the *c*enter*l*ine *t*ube limit diameter (note: $D_{ctl} = D_{otl} - D_t$ where D_t is the outside diameter of the tubes). The *b*affle *c*ut *h*eight is shown as a height L_{bch}; the value of the baffle cut B_c is (L_{bch}/D_s) x 100%, i.e. given in terms of the *percent* of the shell internal diameter. The diametral clearance between the shell internal diameter D_s and outer tube limit diameter D_{otl} is L_{bb}. One-half of L_{bb} is the width of this bypass channel. A pass partition lane is shown with a width of L_p. The diametral clearance between the shell internal diameter D_s and the diameter of the baffle D_b is L_{sb}, where the gap is equal to $L_{sb}/2$.

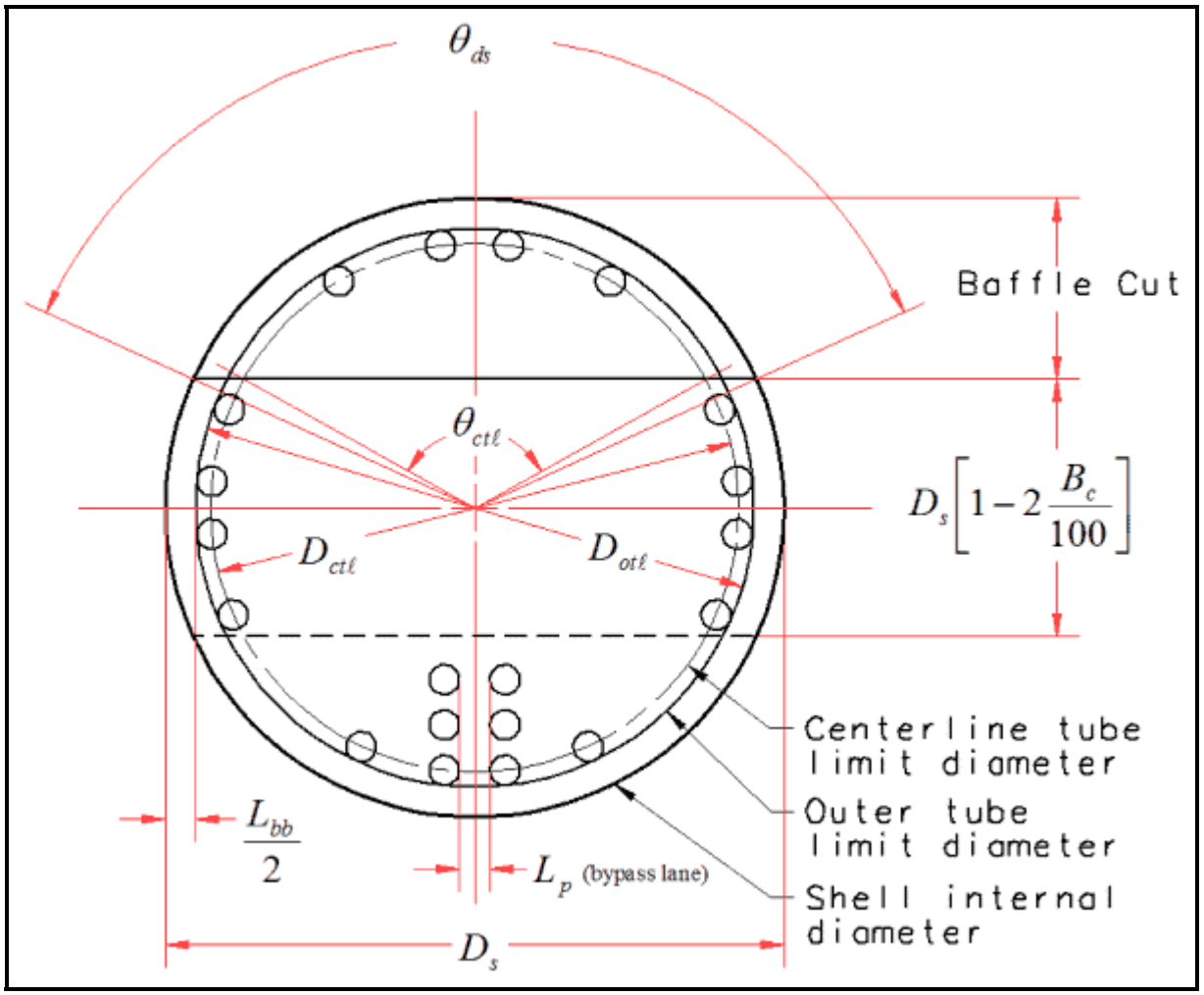

Figure 3.6. Baffle and tube bundle geometry.

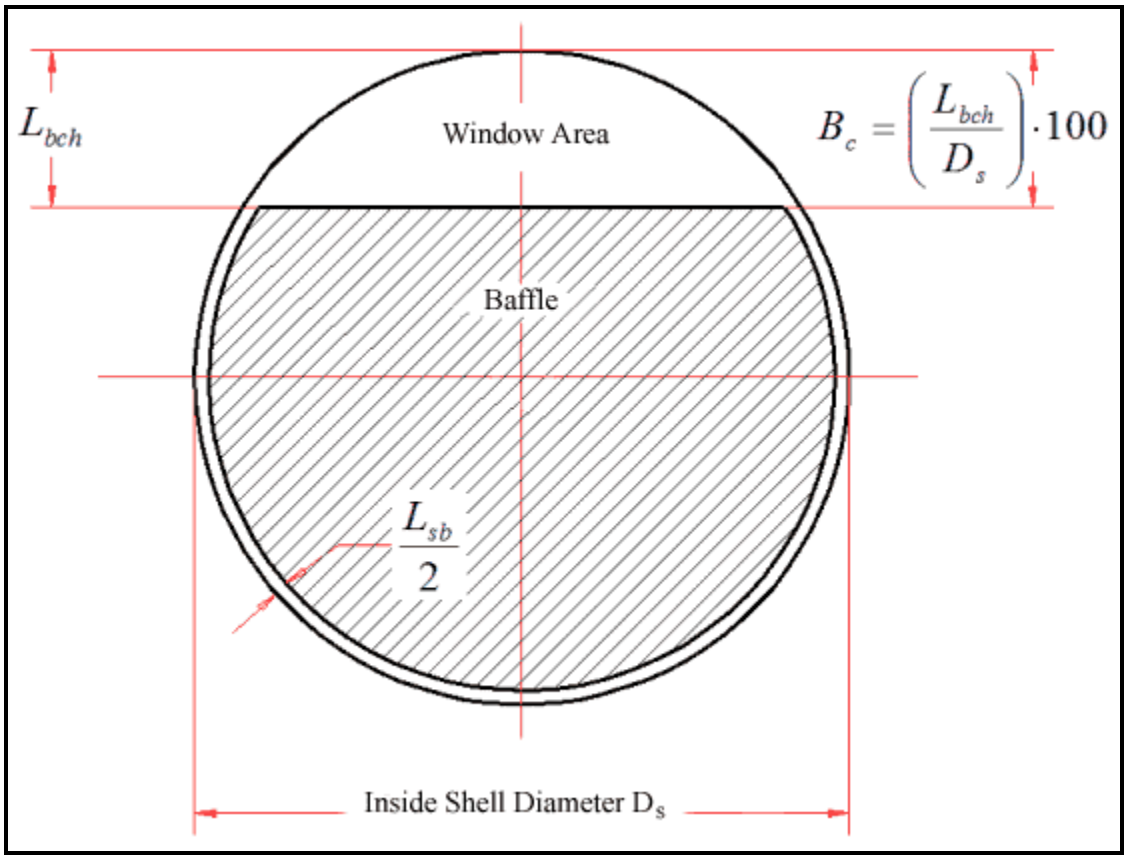

Figure 3.7. Baffle cut and clearance.

The above dimensions D_s, D_{otl}, baffle cut (% of D_s), L_{bb} and L_{sb} can be obtained from a tube layout drawing of the heat exchanger. If the value of D_{otl} is not known, L_{bb} can be assumed to be equal to 9.525 mm (3/8 in.) for D_s < 300 mm (11.81 in.) and L_{bb} can be assumed to be 15.875 mm (5/8 in.) for D_s > 1000 mm (39.37 in.). For D_s from 300 to 1000 mm inclusive, L_{bb} can be assumed to be 12.7 mm (1/2 in.). These values are typical of TEMA heat exchanger specifications but are often smaller for direct-expansion evaporators. If L_{sb} is not known, it can be assumed that L_{sb} = 2.0 mm for D_s < 400 mm (15.75 in.) while for larger shells $L_{sb} = 1.6 + 0.004D_S$ (mm). If the diametral clearance between the baffle holes and the outside of the tube is not known, the maximum TEMA value can be assumed 0.794 mm (1/32 in.) or a smaller value in the range from 0.397 mm (1/64 in.) to 0.794 mm. This clearance is equal to the baffle hole diameter minus D_t. Thermal performance is significantly improved by minimizing this clearance.

The three tube layouts addressed by the Taborek design method are shown in Figure 3.8: 30°, 45° and 90°. The 60° layout is not included. The *t*ube *p*itch is L_{tp} and is defined as the distance center-to-center between tubes in the bundle. The *p*itch *p*arallel to the direction of flow is L_{pp} while that *p*itch *n*ormal to the direction of the flow is L_{pn}.

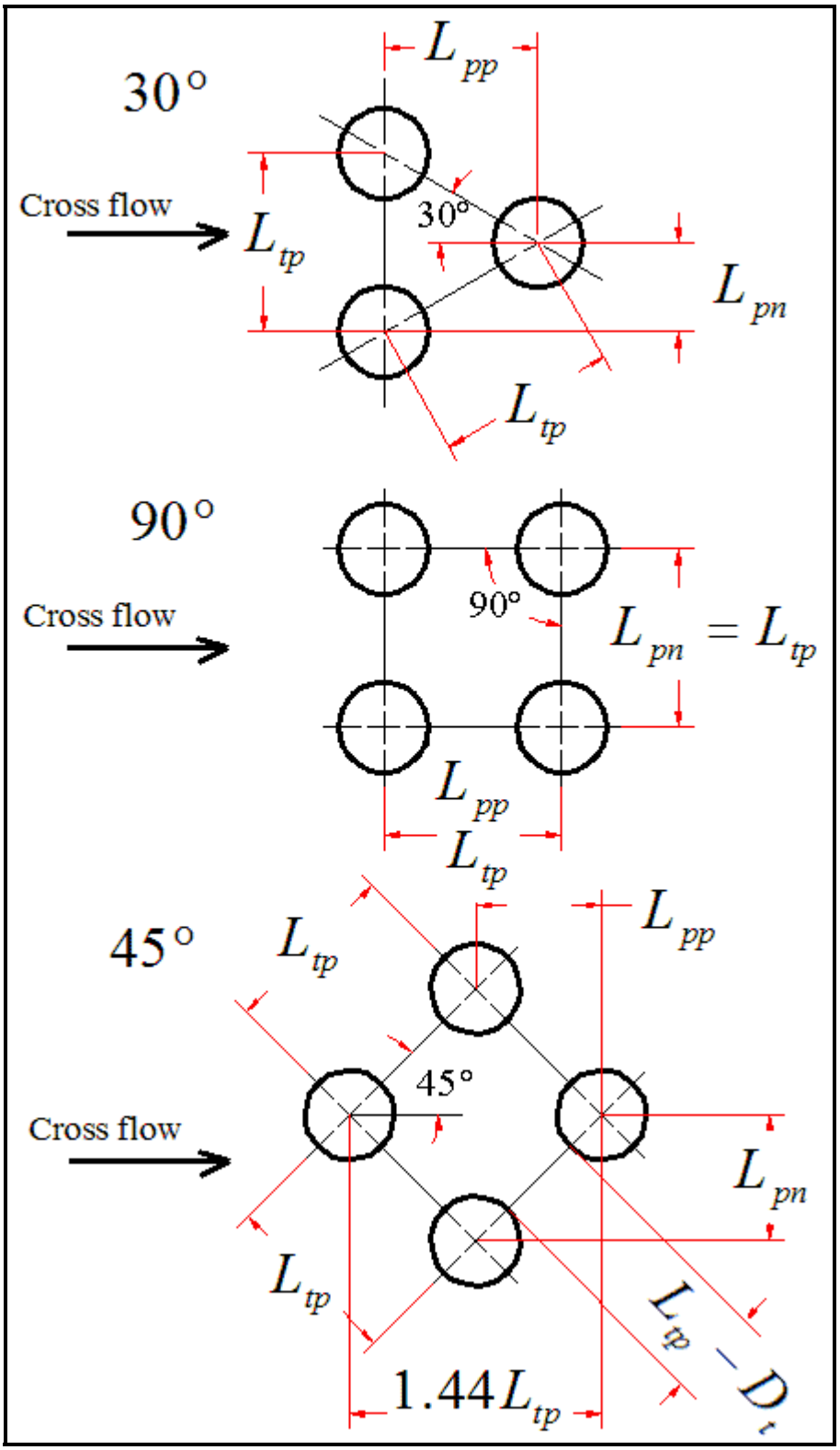

Figure 3.8. Tube layouts.

The number of tubes that fit within a shell depends on a number of geometrical factors, dimensions and clearances, principally the type of tube layout (triangular, square or rotated square) and the tube pitch.

The simple estimation method presented by Taborek (1983) for fixed tubesheets for single tubepass units without any tubes removed in the nozzle entrance and exit areas is:

$$N_{tt} = \frac{0.7854 D_{ctl}^2}{C_1 L_{tp}^2} \qquad [3.3.1]$$

where N_{tt} is the number of tubes, D_{ctl} is the centerline tube limit diameter and L_{tp} is the tube pitch. The constant C_1 = 1.0 for square (90°) and rotated square tube (45°) layouts and C_1 = 0.866 for triangular (30°) tube layouts. Designs with multiple tubepasses (2, 4, …) are commonly used and they will have fewer tubes than given by the above expression. Use of a tube count software program is highly recommended for an accurate estimate since tubes are often removed at the inlet nozzle to permit placement of an impingement plate and the number removed depends on the nozzle diameter. An accurate tube count improves the accuracy of the heat transfer and pressure drop calculations.

3.4 Stream Analysis of Heat Transfer in a Baffled Heat Exchanger

The stream analysis shell-side heat transfer coefficient for single-phase flow α_{ss} is

$$\alpha_{ss} = \left(J_C J_L J_B J_R J_S J_\mu\right)\alpha_I \qquad [3.4.1]$$

where α_I is the ideal tube bank heat transfer coefficient calculated for all the flow across the tube bundle (that is all flow assumed to be in stream B). J_C, J_L, J_B, J_R and J_S are the correction factors for the leakage and bypass flow effects and J_μ is the wall viscosity correction factor. The corrections factors and ideal tube bank heat transfer correlations are described in the sections below. The value of α_{ss} is the mean value for the whole tube bundle applied to the outside heat transfer surface area of the tubes. Mean bulk physical properties are used for evaluating the correlations.

3.4.1 Baffle Cut Correction Factor (J_C)

The baffle cut correction factor J_C accounts for the non-ideal flow effects of window flow on heat transfer since the velocity through the window (that of the baffle cut) is not the same as that for cross-flow over the bundle. The window flow velocity can be larger or smaller than for cross-flow depending on the size of the cut and the baffle spacing. In addition, the window flow is partially longitudinal to the tubes, which is less effective than cross-flow. Therefore, J_C is a function of the baffle cut, the outer tube limit diameter and the window flow area and is calculated as follows:

$$J_C = 0.55 + 0.72 F_C \qquad [3.4.2]$$

where F_C is

$$F_C = 1 - 2F_w \qquad [3.4.3]$$

F_w is the fraction of the cross-sectional area occupied by the window:

$$F_w = \frac{\theta_{ctl}}{360} - \frac{\sin\theta_{ctl}}{2\pi} \qquad [3.4.4]$$

The angle of the baffle cut relative to the *c*en*ter*l*i*ne of the heat exchanger is θ_{ctl} (in degrees):

$$\theta_{ctl} = 2\cos^{-1}\left\{\frac{D_s}{D_{ctl}}\left[1-2\left(\frac{B_c}{100}\right)\right]\right\} \qquad [3.4.5]$$

The above expression is valid for baffle cuts from 15% to 45% of the shell diameter. Use of baffle cuts outside this range is not normally recommended because of the ensuing maldistribution of the flow. J_C typically ranges in value from 0.65 to 1.175 in a well-designed unit.

3.4.2 Baffle Leakage Correction Factor (J_L)

The pressure difference between neighboring baffle compartments forces a fraction of the flow through the baffle-to-tubehole gaps in the baffles (Stream A) and through the annular gap between the shell and the baffle edge (Stream E). These streams reduce the part of the flow that passes over the tube bundle as cross-flow (Stream B), reducing both the heat transfer coefficient *and* the pressure drop. Stream E is very detrimental to thermal design because it is not effective for heat transfer. The baffle leakage correction factor is calculated from the following expression:

$$J_L = 0.44(1-r_s) + [1-0.44(1-r_s)]\exp(-2.2r_{lm}) \qquad [3.4.6]$$

where r_s is

$$r_s = \frac{S_{sb}}{S_{sb}+S_{tb}} \qquad [3.4.7]$$

and r_{lm} is

$$r_{lm} = \frac{S_{sb}+S_{tb}}{S_m} \qquad [3.4.8]$$

The *s*hell-to-*b*affle leakage area S_{sb}, the *t*ube-to-*b*affle hole leakage area S_{tb} for $N_{tt}(1\text{-}F_w)$ tube holes and the cross-flow area at the bundle centerline S_m are determined as follows:

$$S_{sb} = 0.00436 D_s L_{sb}(360-\theta_{ds}) \qquad [3.4.9]$$

$$S_{tb} = \left\{\frac{\pi}{4}\left[(D_t+L_{tb})^2 - D_t^2\right]\right\} N_{tt}(1-F_w) \qquad [3.4.10]$$

$$S_m = L_{bc}\left[L_{bb} + \frac{D_{ctl}}{L_{tp,eff}}(L_{tp}-D_t)\right] \qquad [3.4.11]$$

In the above expressions, L_{sb} is the diametral shell to baffle clearance and the baffle cut angle θ_{ds} in degrees is

$$\theta_{ds} = 2\cos^{-1}\left[1 - 2\left(\frac{B_c}{100}\right)\right] \qquad [3.4.12]$$

where L_{bc} is the central baffle spacing and L_{bb} is the bypass channel diametral gap, both described earlier. The *eff*ective *t*ube *p*itch is $L_{tp,eff}$, which is equal to L_{tp} for 30° and 90° tube layouts while for 45° staggered layouts $L_{tp,eff}$ is equal to $0.707L_{tp}$. For a well-proportioned heat exchanger, J_L > 0.7-0.9 while values of J_L < 0.6 should be avoided. The maximum value of J_L is 1.0. For refrigeration chillers and water-cooled condensers, a value of 0.85 to 0.90 is achievable because of their tighter construction tolerances and smaller clearances than TEMA standards.

3.4.3 Bundle Bypass Correction Factor (J_B)

The bundle bypass correction factor J_B accounts for the adverse effect of the flow between the inner shell wall and the tube bundle (Stream C) and the bypass lane created by any pass partition lanes (Stream F) in the direction of flow. Stream F is not always present and it can be eliminated completely by placing dummy tubes in the pass partition lanes. Stream C is reduced by a tighter fit of the tube bundle into the shell and also by placing sealing strips (in pairs) around the bundle perimeter, up to a maximum of one pair of strips for every two tube rows passed by the flow between the two baffle cuts. The bundle bypass correction factor J_B is

$$J_B = \exp\left[-C_{bh}F_{sbp}\left(1 - \sqrt[3]{2r_{ss}}\right)\right] \qquad [3.4.13]$$

The empirical factor C_{bh} = 1.35 for laminar flow (100 ≥ Re) and C_{bh} = 1.25 for transition and turbulent flows (Re > 100). To evaluate this expression, one requires the ratio of the bypass to the crossflow area F_{sbp}, and the ratio r_{ss} of the number of sealing strips N_{ss} (number of pairs if any) passed by the flow to the number of tube rows crossed between baffle tips in one baffle section N_{tcc}. First of all, F_{sbp} is given by

$$F_{sbp} = \frac{S_b}{S_m} \qquad [3.4.14]$$

where S_m was given above and S_b is the bypass area:

$$S_b = L_{bc}\left[\left(D_s - D_{otl}\right) + L_{pl}\right] \qquad [3.4.15]$$

where L_{pl} represents the width of the bypass lane between tubes. For situations without a pass partition lane or for such a lane normal to the flow direction, set L_{pl} = 0 while for a pass partition lane parallel to the flow direction L_{pl} is equal to ½ the actual dimension of the lane or can be assumed to be equal to the tube diameter D_t. The ratio r_{ss} is

$$r_{ss} = \frac{N_{ss}}{N_{tcc}} \qquad [3.4.16]$$

The value of N_{tcc} is obtained from

$$N_{tcc} = \frac{D_s}{L_{pp}}\left[1 - 2\left(\frac{B_c}{100}\right)\right] \qquad [3.4.17]$$

where $L_{pp} = 0.866L_{tp}$ for a 30° layout, $L_{pp} = L_{tp}$ for a 90° layout and $L_{pp} = 0.707L_{tp}$ for a 45° layout. This expression has a maximum limit of $J_B = 1$ at $r_{ss} \geq ½$.

3.4.4 Unequal Baffle Spacing Correction Factor (J_S)

The unequal baffle spacing correction factor J_S accounts for the adverse effect of an inlet baffle spacing L_{bi} and/or outlet baffle spacing L_{bo} larger than the central baffle spacing L_{bc}. Some exchangers have a larger baffle spacing in the inlet and outlet nozzle compartments compared to the central baffle spacing, allowing placement of the shell-side nozzles without interference with the body flanges and without overlapping the first baffle. The flow velocity in these compartments is thus lowered and has an adverse influence on heat transfer. For larger inlet and outlet spacings than the central baffle spacing, the correction factor $J_S < 1.0$. For inlet and outlet baffle spacings equal to the central baffle spacing, no correction is required and $J_S = 1.0$. The value for J_S is determined directly from the effect on the flow velocity and is given by the following expression:

$$J_S = \frac{(N_b - 1) + (L_{bi}/L_{bc})^{1-n} + (L_{bo}/L_{bc})^{1-n}}{(N_b - 1) + (L_{bi}/L_{bc}) + (L_{bo}/L_{bc})} \qquad [3.4.18]$$

where n = 0.6 for turbulent flow and n = 1/3 for laminar flow. The number of baffle compartments N_b is determined from the effective tube length and the baffle spacings.

3.4.5 Laminar Flow Correction Factor (J_R)

In laminar flows, heat transfer is reduced by the adverse temperature gradient formed in the boundary layer as the flow thermally develops along the flow channel. The laminar flow correction factor J_R accounts for this effect. For laminar shell-side flow $J_R < 1.0$ (i.e. for $100 \geq Re$) while for $Re > 100$, no correction is needed and $J_R = 1.0$. For $20 \geq Re$, the value of J_R is given by

$$J_R = (J_R)_{20} = \left(\frac{10}{N_c}\right)^{0.18} \qquad [3.4.19]$$

where N_c is the total number of tube rows crossed by the flow in the entire heat exchanger:

$$N_c = (N_{tcc} + N_{tcw})(N_b + 1) \qquad [3.4.20]$$

The number of tuberows crossed N_{tcc} between baffle tips has been noted above while the number of tube rows crossed in the window area N_{tcw} is

$$N_{tcw} = \frac{0.8}{L_{pp}}\left[D_s\left(\frac{B_c}{100}\right) - \frac{D_s - D_{ctl}}{2}\right] \qquad [3.4.21]$$

For $Re > 20$ but $Re < 100$, the value is prorated as

$$J_R = (J_R)_{20} + \left(\frac{20 - Re}{80}\right)\left[(J_R)_{20} - 1\right] \qquad [3.4.22]$$

The minimum value of J_R in all cases is 0.4.

3.4.6 Wall Viscosity Correction Factor (J_μ)

Heat transfer and pressure drop correlations are normally evaluated using bulk physical properties obtained at the mean of the inlet and outlet temperatures. For heating and cooling of liquids, the effect of variation in properties between the bulk fluid temperature and the wall temperature is corrected by the viscosity ratio J_μ, which is the ratio of the bulk viscosity μ to the wall viscosity μ_{wall}:

$$J_\mu = \left(\frac{\mu}{\mu_{wall}}\right)^m \qquad [3.4.23]$$

The correction factor is greater than 1.0 for heating the shell-side fluid and vice-versa for cooling the shell-side fluid. The exponent for heating and cooling of liquids is usually set to m = 0.14. For gases, no correction is required for a gas being cooled while a correction based on temperature rather than viscosity is used for gases being heated as follows:

$$J_\mu = \left(\frac{T + 273}{T_{wall} + 273}\right)^{0.25} \qquad [3.4.24]$$

where T is the bulk temperature and T_{wall} is the wall temperature. The wall temperature must be calculated from a preliminary heat transfer calculation to determine the viscosity at the wall.

3.4.7 Ideal Tube Bank Heat Transfer Coefficient (α_I)

The ideal tube bank heat transfer coefficient α_I is calculated for all the flow across the tube bundle (that is as if all the flow in the exchanger were in Stream B without any bypass flows) as:

$$\alpha_I = j_I c_p \dot{m} Pr^{-2/3} \qquad [3.4.25]$$

The mass velocity of the fluid $\dot{m}$ is based on the total flow M through the minimum flow area normal to the flow and is in units of kg/m^2s. Pr is the Prandtl number. The heat transfer factor j_I is obtained as follows:

$$j_I = a_1\left(\frac{1.33}{L_{tp}/D_t}\right)^a Re^{a_2} \qquad [3.4.26]$$

$$a = \frac{a_3}{1 + 0.14 Re^{a_4}} \qquad [3.4.27]$$

The values of a_1, a_2, a_3 and a_4 are listed in Table 3.1 given by Taborek (1983). For the above methods, the shell-side cross-flow mass velocity at the maxumum cross-section of the tube bundle is

$$\dot{m} = \frac{M}{S_m} \qquad [3.4.28]$$

where M is the shell-side flow rate in kg/s and S_m was defined earlier. The shell-side Reynolds number is then

$$Re = \frac{D_t \dot{m}}{\mu} \qquad [3.4.29]$$

The Prandtl number is defined as

$$Pr = \frac{c_p \mu}{k} \qquad [3.4.30]$$

The physical properties (viscosity μ, specific heat c_p and thermal conductivity k) are evaluated at the mean bulk fluid temperature. The effective tube length L_{ta} is used to calculate the actual heat transfer surface area A_o as

$$A_o = \pi D_t L_{ta} N_{tt} \qquad [3.4.31]$$

for the number of tubes in the bundle N_{tt}.

Table 3.1. Empirical coefficients for calculation of j_I and f_I.

Layout	Re	a_1	a_2	a_3	a_4	b_1	b_2	b_3	b_4
30°	10^5-10^4	0.321	-0.388	1.450	0.519	0.372	-0.123	7.00	0.500
	10^4-10^3	0.321	-0.388			0.486	-0.152		
	10^3-10^2	0.593	-0.477			4.570	-0.476		
	10^2-10	1.360	-0.657			45.10	-0.973		
	<10	1.400	-0.667			48.00	-1.000		
45°	10^5-10^4	0.370	-0.396	1.930	0.500	0.303	-0.126	6.59	0.520
	10^4-10^3	0.370	-0.396			0.333	-0.136		
	10^3-10^2	0.730	-0.500			3.500	-0.476		
	10^2-10	0.498	-0.656			26.20	-0.913		
	<10	1.550	-0.667			32.00	-1.000		
90°	10^5-10^4	0.370	-0.395	1.187	0.370	0.391	-0.148	6.30	0.378
	10^4-10^3	0.107	-0.266			0.0815	+0.022		
	10^3-10^2	0.408	-0.460			6.0900	-0.602		
	10^2-10	0.900	-0.631			32.100	-0.963		
	<10	0.970	-0.667			35.000	-1.000		

3.5 Stream Analysis of Shell-Side Pressure Drop in a Baffled Heat Exchanger

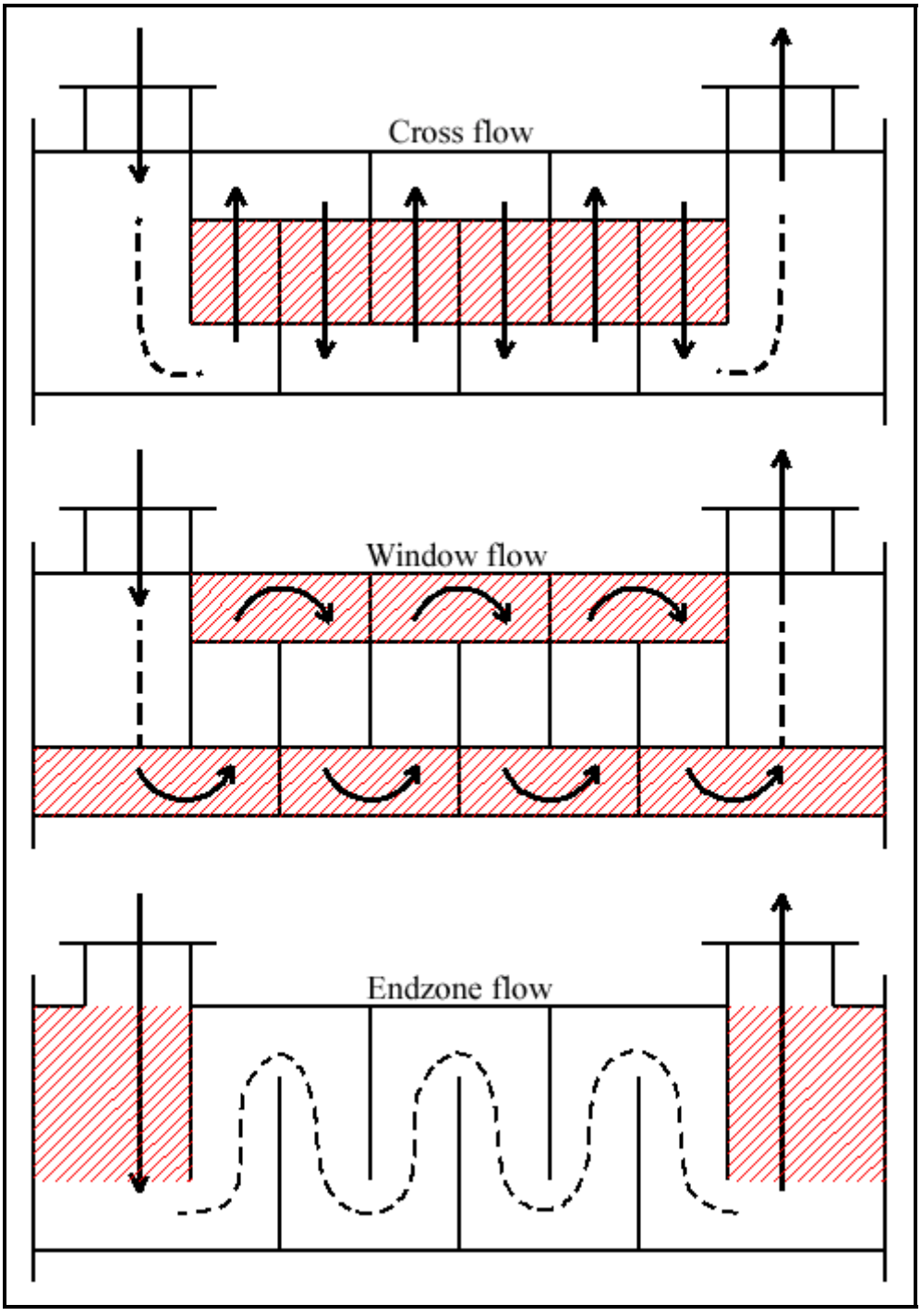

Figure 3.9. Pressure drop regions in shell-side flow.

The pressure drop for shell-side flow is equal to the sum of the inlet nozzle pressure drop, the bundle pressure drop and the outlet nozzle pressure drop. The inlet and outlet nozzle pressure drops can be

approximated as being equal to 2 velocity heads each. The bundle pressure drop is equal to the sum of the cross-flow pressure drops Δp_c, the window pressure drops Δp_w, and the two end zone pressure drops (first and last baffle compartments) Δp_w as illustrated in Figure 3.9. The bundle pressure drop Δp_{total}, excluding nozzles or impingement plates, is

$$\Delta p_{total} = \Delta p_c + \Delta p_w + \Delta p_e \qquad [3.5.1]$$

The pressure drop Δp_c across tube bundle between the baffle tips is based on the ideal tube bank pressure drop Δp_{bI} for one baffle compartment with the central baffle spacing L_{bc}. The zones covered by this pressure drop are the central baffle compartments for flow between the baffle cuts. The pressure drop in all the central baffle compartments (N_b-1) is

$$\Delta p_c = \Delta p_{bI}(N_b - 1)R_B R_L \qquad [3.5.2]$$

where Δp_{bI} is the ideal bundle pressure drop for one baffle compartment of the N_b compartments and is based on the mass velocity defined earlier. The expression for Δp_{bI} is:

$$\Delta p_{bI} = 0.002 f_I N_{tcc} \frac{\dot{m}^2}{\rho} R_\mu \qquad [3.5.3]$$

The friction factor f_I is obtained from

$$f_I = b_1 \left(\frac{1.33}{L_{tp}/D_t} \right)^b Re^{b_2} \qquad [3.5.4]$$

where

$$b = \frac{b_3}{1 + 0.14 Re^{b_4}} \qquad [3.5.5]$$

The empirical constants for b, b_1, b_2, b_3 and b_4 are taken from Table 3.1. The viscosity correction factor R_μ on pressure drop is

$$R_\mu = \left(\frac{\mu}{\mu_w} \right)^{-m} \qquad [3.5.6]$$

The values of m were cited earlier. The bypass correction factor R_B is

$$R_B = \exp\left[- C_{bp} F_{sbp} \left(1 - \sqrt[3]{2 r_{ss}} \right) \right] \qquad [3.5.7]$$

with the limit of $R_B = 1$ for $r_{ss} \geq ½$ while F_{sbp} was defined earlier. For the empirical factor C_{bp}, use C_{bp} = 4.5 for laminar flow ($100 \geq Re$) and C_{bh} = 3.7 for transition and turbulent flows ($Re > 100$). The leakage correction factor R_L is

$$R_L = \exp\left[- 1.33 (1 + r_s) r_{lm}^p \right] \qquad [3.5.8]$$

where r_s and r_{lm} were defined earlier and the exponent p is

$$p = -0.15(1 + r_s) + 0.8 \quad [3.5.9]$$

The pressure drop and mass velocity in all N_b window zones for turbulent flow (Re > 100) are

$$\Delta p_w = N_b \left[(2 + 0.6 N_{tcw}) \frac{0.001 \dot{m}_w^2}{2\rho} \right] R_L R_\mu \quad [3.5.10]$$

$$\dot{m}_w = \frac{M}{\sqrt{S_m S_w}} \quad [3.5.11]$$

where M is the shell-side flow rate in kg/s. The areas S_m and S_w are found from their appropriate expressions presented earlier. The 0.6 in the above expression accounts for the frictional effects and the factor 2 accounts for the velocity heads for the flow turnaround in the window. For laminar flow (100 ≥ Re), the equivalent expression is

$$\Delta p_w = N_b \left\{ 26 \left(\frac{\dot{m}_w \mu}{\rho} \right) \left[\frac{N_{tcw}}{L_{tp} - D_t} + \frac{L_{bc}}{D_w^2} \right] + \left[\frac{0.002 \dot{m}_w^2}{2\rho} \right] \right\} R_L R_\mu \quad [3.5.12]$$

The first term in brackets refers to the cross flow and the second term refers to the longitudinal flow. The hydraulic diameter of the baffle window is

$$D_w = \frac{4 S_w}{\pi D_t N_{tw} + (\pi D_s \theta_{ds} / 360)} \quad [3.5.13]$$

θ_{ds} was defined earlier. N_{tw} is the number of tubes in the window and is determined from the total number of tubes N_{tt} as

$$N_{tw} = N_{tt} F_w \quad [3.5.14]$$

where F_w was defined earlier. S_w is the net flow area in the window, given as

$$S_w = S_{wg} - S_{wt} \quad [3.5.15]$$

The area occupied by the N_{tw} tubes in the window is S_{wt} and is calculated as

$$S_{wt} = N_{tw} \left(\frac{\pi}{4} D_t^2 \right) \quad [3.5.16]$$

The gross window flow area without tubes in the window is S_{wg}, given as

$$S_{wg} = \frac{\pi D_s^2}{4}\left(\frac{\theta_{ds}}{360} - \frac{\sin\theta_{ds}}{2\pi}\right) \qquad [3.5.17]$$

The pressure drop Δp_e in the two end zones of the tube bundle is

$$\Delta p_e = \Delta p_{bI}\left(1 + \frac{N_{tcw}}{N_{tcc}}\right)R_B R_S \qquad [3.5.18]$$

The pressure drop correction for unequal baffle spacings at the inlet and/or outlet with respect to the central baffle spacing is R_S, calculated as follows:

$$R_S = \left(\frac{L_{bc}}{L_{bo}}\right)^{2-n} + \left(\frac{L_{bc}}{L_{bi}}\right)^{2-n} \qquad [3.5.19]$$

The tube numbers N_{tcw} and N_{tcc} were defined earlier as were methods for calculating Δp_{bI}, R_B and R_μ. For all baffle spacings of equal length, $R_S = 2$. In the above expression, N = 1 for laminar flow (Re < 100) and n = 0.2 for turbulent flow.

3.6 Stream Analysis Applied to Low Finned Tube Bundles

In this section, the above plain tube method is applied to integral low finned tube bundles using the modifications proposed by Taborek (1983).

3.6.1 Low Finned Tubes and Applications

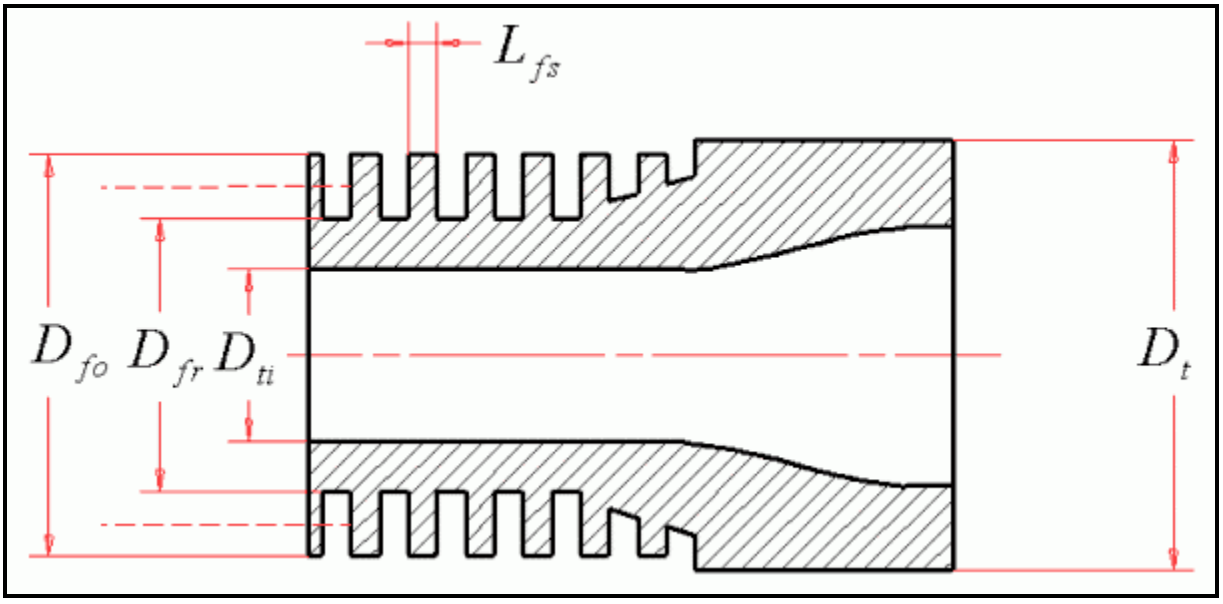

Figure 3.10. Geometric description of integral low finned tube.

Low finned tubes are an excellent heat transfer enhancement to apply to single-phase shell-side flows, for both liquid flows and even more so for gas flows. Figure 3.10 shows a geometric sketch of an integral low

finned tube that is defined by its following dimensions. The characteristic dimensions are: tube diameter at the plain unfinned end D_t, the tube diameter of the fin tips D_{fo} (typically equal to D_t), the root diameter at the base of the fins D_{fr}, the tube internal diameter in the finned zone D_{ti}, the fin thickness L_{fs}, the number of fins per meter N_f and finally the actual wetted surface area per unit length A_{of}. Figure 3.11 shows a photograph of a selection of Wolverine Tube low finned tubes. Integral low finned tubes are available in nearly every common heat exchanger tube material. Common fin densities range from 630 to over 1000 fins per meter (commonly defined as their number of fins per inch, such as 19 fpi, 26 fpi, 28 and 30 fpi tubes). Typically fin heights are up to about a maximum of 1.5 mm (0.059 in.) while fin thickness is commonly about 0.3 mm (0.012 in.). Tables of integral low finned tubes with their dimensions are available from the Wolverine Tube Inc. website.

Figure 3.11. A selection of low finned tubes of Wolverine Tube Inc.

For many single-phase flows, it is advantageous to use integral low finned tubes rather than plain tubes. Low finned tubes are appropriate for applications where the shell-side (outside) heat transfer coefficient is small compared to the tube-side coefficient and/or when the shell-side fouling factor is controlling the design. The first situation most often occurs (a) when the shell-side flow is at the low end of the turbulent flow regime, in the transition regime or in the laminar flow regime, (b) when the allowable pressure drop is small, requiring use of large baffle cuts and baffle spacings, or (c) when a heat transfer augmentation is used on the inside of the tube, such as helical fins or ribs inside Wolverine Tube low finned tubes.

Another very important benefit of low finned tubes is their positive effect on the shell-side *fouling resistance*. Since the shell-side *fouling factor* is applied to the total wetted surface area (which is about 3 to 4 times that of a plain tube), the effective fouling resistance is reduced by a factor of 3 to 4 using the same fouling factor value as for the plain tube design. For large fouling factors or where the fouling resistance is significant (quite typical situation even for modest fouling factor values), the effect of the large surface area ratio of a low finned tube can dramatically increase the overall heat transfer coefficient. Hence, one uses a low finned tube to increase the shell-side heat transfer coefficient, to decrease the shell-side fouling resistance and to increase the tube-side velocity and heat transfer coefficient (also D_{ti} is less than that of the plain ends of the tube).

It is important to remember that when an external low finned tube is used, the internal diameter of the finned section of the tube D_{ti} should be used for determining the tube-side heat transfer coefficient and pressure drop. The most effective low finned tube geometry can be determined by trying several different fin densities. If corrosion allowances are important, thick fins should be used. For large corrosion allowances, fins may not be appropriate since they may be worn away.

3.6.2 Heat Transfer and Pressure Drops with Low Finned Tubes

The stream analysis method of Taborek (1983) for *plain tubes* was extended by Taborek in the same publication to application to *integral low finned tube bundles*. The changes to the above design equations are presented below. The heat transfer coefficient for the shell-side of a low finned tube bundle is used to

then calculate the overall heat transfer coefficient, at which point the fin efficiency of the low fins must be taken into account.

Input data. The following additional information is required for calculating the shell-side thermal performance of a low finned tube bundle:

Diameter over the fins:	D_{fo}
Fin root diameter:	D_{fr}
Number of fins per unit of tube length:	N_f
Average fin thickness (assuming rectangular profile):	L_{fs}
Wetted surface area of finned tube per unit of tube length:	A_{of}
Tube-to-baffle hole clearance:	L_{tb}

To determine L_{tb}, use D_{fo} in place of D_t. Normally, D_{fo} is equal to or slightly less than D_t.

Heat transfer and flow geometries.

The total heat transfer surface area upon which to apply the shell-side heat transfer coefficient of the finned tube bundle α_{ss} is A_o, which for the finned tube is obtained from the following expression:

$$A_o = A_{of} L_{ta} N_{tt} \qquad [3.6.1]$$

The equivalent projected area of an integral low finned tube is less than that of a plain tube of the same diameter because of the openings between adjacent fins in the direction of flow. Hence, the "melt down" or equivalent projected diameter D_{req} is a function of the tube geometry and density as:

$$D_{req} = D_{fr} + 2L_{fh} N_f L_{fs} \qquad [3.6.2]$$

and the fin height L_{fh} is

$$L_{fh} = \frac{D_{fo} - D_{fr}}{2} \qquad [3.6.3]$$

Thus, wherever the plain tube diameter D_t appeared in the correlations and geometrical equations for the plain tube bank, it is replaced by D_{req} or as noted below:

S_m calculations: use D_{req} in place of D_t.
Re calculation: use D_{req} in place of D_t.
S_{wt} calculation: use D_{fo} in place of D_t.

Ideal tube bank values of j_I.

The method for plain tubes is applicable to low finned tubes without modification with Re determined using D_{req} rather than D_t for Re >1000. When Re < 1000, a laminar boundary layer overlap on the fins begins to adversely affect the heat transfer. This is accounted for by the following expression, applicable only when Re <1000:

$$j_I = J_f j_{I,plain} \qquad [3.6.4]$$

In Taborek (1983), a graph is given for the variation in J_f versus log Re from Re = 20 to Re = 1000, where $J_f = 1.0$ at Re = 1000. This curve has been fitted here as follows:

$$J_f = 0.58 + 0.42\left(\frac{\log(Re/20)}{\log(1000/20)}\right) \qquad [3.6.5]$$

Ideal tube bank values of f_I.

The equivalent cross-flow area is larger for a finned tube bundle relative to an identical plain tube bundle because of the additional flow area between the fins. For finned tubes the friction factor is about 1.4 times larger than for a plain tube; however, the lower velocity due to the larger flow area from the open area between fins in the direction of flow is also taken into account in the Reynolds number Re. To calculate the friction factor for the low finned tube bank, first calculated $f_{I,plain}$ using the finned tube values of Re and D_{req} from the plain tube correlation and then multiply this value by 1.4 as follows:

$$f_I = 1.4 f_{I,plain} \qquad [3.6.6]$$

Example calculation: a detailed six-page example calculation is available in Taborek (1983) that is recommended to the reader.